Supporting Information

In Search of Novel CDK8 Inhibitors by Virtual Screening

Malika Kumarasiri,[†¶] Theodosia Teo,[†¶] Mingfeng Yu,[¶] Stephen Philip,[¶] Sunita K. C. Basnet,[¶] Hugo Albrecht,[¶] Matthew J. Sykes,[¶] Peng Wang,[§] Shudong Wang*[¶]

[¶]Centre for Drug Discovery and Development, Sansom Institute for Health Research, Centre for Cancer Biology, and School of Pharmacy and Medical Sciences, University of South Australia, Adelaide, South Australia 5001, Australia

[§]Yabao Pharmaceutical Group Co., Ltd., Suzhou Industrial Park, Suzhou, China, 215123

Corresponding Author

*Phone: +61 8 8302 2372. Email: shudong.wang@unisa.edu.au.

Author Contributions

[†]These authors contributed equally.

CDK8 BIOLOGY

CDK8/CycC negatively regulates transcription by mediating the activity of CDK7/CycH, which, in turn, represses the initiation of transcription.[1] Conversely, it has also been shown that CDK8 can act as a positive regulator in the transcription of specific genes.[2-6] CDK8 is overexpressed in a variety of cancers including melanoma, breast, colorectal and pancreatic cancers.[7-10] CDK8 inhibition also produces potent anti-proliferative effects in acute myeloid leukemia (AML) cells.[11] *CDK8* is deemed an oncogene in colorectal cancers. Genetic knockout of CDK8 has been shown to restrain proliferation, metastasis, and invasion of colon cancer cells *in vitro* and *in vivo*.[12-14] Importantly, inhibition of CDK8 has been shown to escalate the native activities of Natural Killer cells, promoting their tumor surveillance and cytotoxicity.[15] Furthermore, murine models have been used to demonstrate that CDK8 inhibition is dispensable for normal cell growth.[16]

Significant work has been done to assess deregulation of the Wnt/β-catenin signaling pathway by way of CDK8, in colorectal cancers.[17-19] Firestein and co-workers identified that CDK8 has a direct and positive role in regulating the β-catenin-driven oncogenic transformation, in which knockdown of CDK8 significantly decreased β-catenin-dependent transcriptional activity.[12] In addition, CDK8 positively mediates β-catenin-stimulated transcription through inhibiting E2F1, a β-catenin antagonist.[14] Therefore, inhibiting CDK8 in colorectal cancers is highly likely be of clinical value. In fact, proliferation of colon cancer cells with high CDK8 expression levels has been demonstrated to be suppressed by CDK8 depletion.[12]

METHODS

Compound databases. An initial search led to the choice of ChemBridge and ChemDiv drug-like molecule databases. These databases are frequently used throughout the literature for virtual screening and the compounds are readily purchasable. The total number of compounds in the two databases was ~2.1 million (as of 16 Sep 2015). All compounds were filtered through FILTER *v*2.0.2[20, 21] using the following criteria: (1) molecular weight: 150 to 600 g/mol, (2) logarithm of the partition coefficient (XlogP): -4 to +6, (3) net charge: -3 to +3, (4) rotatable bond: 1 to 8, (5) polar surface area: 0 to 200 $Å^2$, (6) hydrogen bond donor: 0 to 10, and (7) hydrogen bond acceptor: 0 to 10. 3D conformations of the

filtered compounds were generated using OMEGA *v*2.4.6,[21, 22] resulting in two libraries of 1,138,206 (ChemBridge) and 1,024,000 (ChemDiv) molecules.

Homology modeling. Existing CDK8 X-ray crystal structures have unresolved regions in the vicinity of the ATP-binding site. Thus, homology modeling was used to generate two complete and optimal structural models; one in the DMG-in conformation and the other in the DMG-out conformation. The sorafenib-bound CDK8/CycC crystal structure (PDB ID: 3RGF) was used as the template for the DMG-out model, while a structure of CDK8/CycC with a Senexin A analog (PDB ID: 4F7S) bound was employed for the DMG-in model. 100 homology models were generated for each conformation using Modeller *v*9.12,[23] and the top scoring models were found to have high similarities when ranked according to their DOPE scores.[24] A top scoring model for each conformation was selected upon inspection of backbone and side chain conformation, and was energy-minimized using Amber 14 with the FF14SB and GAFF forcefields.[25]

Virtual screening cascades. Two complementary virtual screening cascades were employed to identify type I (binds to DMG-in) and type II (targets DMG-out) CDK8 inhibitors. One cascade was biased to five known CDK8 inhibitor structures, while the other was unbiased. In the biased screening protocol, the OpenEye vROCS *v*3.1.2[26, 27] program was used to search for potential CDK8 inhibitors based on structural similarity with sorafenib, Senexin A, SNX-2-165 (2 conformers), ABT869, and AST-487. 240,000 compounds resulted from this and were sequentially fed into FRED *v*3.0.0[28-31] and HYBRID *v*3.0.0,[28-31] producing a total of 29,134 compounds. In the unbiased protocol, both compound libraries were subjected to the HTVS protocol of Schrödinger Glide *v*6.3 against two CDK8 homology models, generating ~15,000 compounds for each type.[32, 33]

The top 30,000 compounds (15,000 × 2 above) obtained from the HTVS and the remaining 29,134 molecules from the biased screening cascade were subjected to Glide SP mode docking using the two CDK8 homology models (*i.e*. four separate calculations). The resulting molecules were then subjected to Glide XP refinement. Finally, the surviving molecules from both cascades were categorized according to the inhibitor type, and were subsequently clustered and analyzed with Schrödinger Canvas to visualize structural diversity.[34, 35]

Cell culture. The colorectal cancer cell lines, Colo 205, HCT 116 and HT-29, were obtained from the cell bank at the Centre for Drug Discovery and Development, University of South Australia. They were cultured in Roswell Park Memorial Institute (RPMI)-1640 tissue culture medium (Sigma Aldrich, Castle Hill, NSW, Australia) with 10% fetal bovine serum (Thermo Fisher Scientific, Scoresby, VIC, Australia) and incubated in a humidified 37 °C, 5% CO_2 incubator.

Chemical, substrates and proteins. Senexin A was synthesized by Le Sun Pharmaceuticals (JiangSu, China) and sorafenib purchased from AdooQ® Bioscience (Irwin, CA, USA). Both compounds were used as positive controls for kinase activity assays. All of the hit compounds, including those originating from the ChemDiv database, were purchased from ChemBridge Corporation (San Diego, CA, USA) with a stated purity of ≥ 95% by NMR and LC-MS. All compounds were prepared as 10 mM stock solutions in 100% DMSO and stored at -20 °C. RBER-IRStide substrate (0.743 µg/µL) and the CDK8/CycC recombinant protein kinase (0.262 µg/µL) were purchased from ProQinase (Freiburg, Germany) and stored as aliquots of 10 µL in heat-resistant vials at -80 °C.

^{33}PanQinase® activity assay. Inhibition of CDK8/CycC upon incubation with each hit identified by virtual screening was measured using a radiometric ^{33}PanQinase® activity assay by ProQinase GmbH (Freiburg, Germany). The assay was performed in 96-well FlashPlates (PerkinElmer, Boston, MA, USA) in a reaction volume of 50 µL. Each well contained 20 µL of assay buffer (70 mM HEPES-NaOH pH 7.5, 3 mM $MgCl_2$, 3 mM $MnCl_2$, 3 µM sodium orthovanadate, 1.2 mM DTT, 50 µg/mL $PEG_{20,000}$), 5 µL of tested compound in 10% DMSO, 20 µL of enzyme/substrate mix (50 ng CDK8/CycC and 1 µg RBER-IRStide total) and 5 µL of 1 µM ATP solution containing approximately 9×10^5 cpm/well [γ-^{33}P]-ATP. The plate was incubated at 30 ºC for an hour, and the reaction was stopped with 50 µL of 2% H_3PO_4. Following a two-step washing with 200 µL of 0.9% NaCl, incorporation of $^{33}P_i$ was determined with a Wallac MicroBeta® microplate scintillation counter. The residual kinase activities at 1 or 10 µM compound concentration were reported as relative activities (%) of average 0 and 100% controls. Final DMSO concentrations were routinely adjusted to 1%.

ADP-Glo kinase assay. The assay was performed in a white polystyrene 96-well plate (Sigma Aldrich, Castle Hill, NSW, Australia) using an ADP-Glo assay kit (Promega Corporation, Auburn, VIC,

Australia) according to the manufacturer's protocols. For the primary screening at a compound concentration of 1 µM, 1 µL of a 10 µM compound solution (5% DMSO) was added to the kinase reaction mixture. For IC_{50} determination, each compound was prepared with a three-fold serial dilution in 100% DMSO ranging from 2 mM to 0.1 µM, followed by 20× dilution into H_2O (5% DMSO). An additional 10× dilution was achieved through final addition of 1 µL to the kinase reaction (see below). The kinase mixture was made up of 3 µL standard assay buffer (167 mM HEPES-NaOH at pH 7.5, 10 mM $MgCl_2$, 10 mM $MnCl_2$, 10 µM sodium orthovanadate and 3.33 mM DTT), 1.5 µL kinase dilution buffer (50 mM HEPES-NaOH at pH 7.5, 0.25 mg/mL $PEG_{20,000}$ and 1 mM DTT) containing 80 ng of CDK8/CycC recombinant protein kinase, 2.5 µL 50 mM HEPES containing 0.24 µg RBER-IRStide substrate. Finally, 2 µL of ATP (19.5 µM) and 1 µL of tested compound were added to reach a total assay volume of 10 µL. The kinase reaction was performed as follows: (1) kinase reaction step at 37 ºC for 40 min following the addition of ATP; (2) an ATP depletion step at room temperature for 40 min by ADP-Glo reagent; and (3) an ADP-to-ATP conversion step in a dark room for 1 hour by kinase detection reagent. Finally, luminescence was quantified using an EnVision® multi-label plate reader (PerkinElmer, Beaconsfield, Buckinghamshire, UK) with an integration time of 1 sec per well. Positive and negative controls were also performed in 5% DMSO in the presence and absence of CDK8/CycC kinase, respectively.

PAINS filtering. The nine hits that showed good inhibition activities in the radiometric and ADP-Glo assays were subjected PAINS filtering[36] using Schrödinger Canvas and PAINS1, PAINS2, and PAINS3 filter groups, which consisted of 409, 55, and 16 filters, respectively. The min and max values were kept at 1 and 2, respectively.

ChEMBL comparison. ChEMBL was searched for entries listed as CDK8 inhibitors. The search resulted in 422 unique entries. The structures of each of the nine hits were compared to these using Schrödinger Canvas, by calculating the Tanimoto similarities. Then, the most similar ChEMBL CDK8 entry was extracted for each of the nine hits.

Tetrazolium-based cell viability assay. The viability of colorectal cancer cells was studied using the 3-(4,5-dimethylthiazol-2-yl)-2,5-diphenyltetrazolium bromide (MTT) (Thermo Fisher Scientific,

Scoresby, VIC, Australia) assay as previously reported.[37] Compound concentrations required to inhibit 50% of cell growth were calculated using non-linear regression analysis by Microsoft Excel. This assay was performed in triplicate and repeated at least twice where the mean ± standard deviation of GI_{50} was obtained.

Western blotting. Western blotting was performed as previously described.[37] Antibodies used were as follows: phosphorylated STAT1 at Ser727 (p-$STAT1^{S727}$), STAT1 and GAPDH (Cell Signaling Technology, Danvers, MA, USA). The anti-rabbit immunoglobulin G (IgG) horseradish peroxidase (HRP)-conjugated secondary antibody was also obtained from Cell Signaling Technology. Enhanced chemiluminescence (ECL) reagents were purchased from GE Healthcare Life Sciences (Rydalmere, NSW, Australia).

Data analysis. Microsoft Excel (Redmond, Washington, USA) or GraphPad Prism version 6.0 (San Diego, CA, USA) was used for data analysis. IC_{50} values were determined through performing curve fitting, and calculated using a four-parameter logistic non-linear regression model.

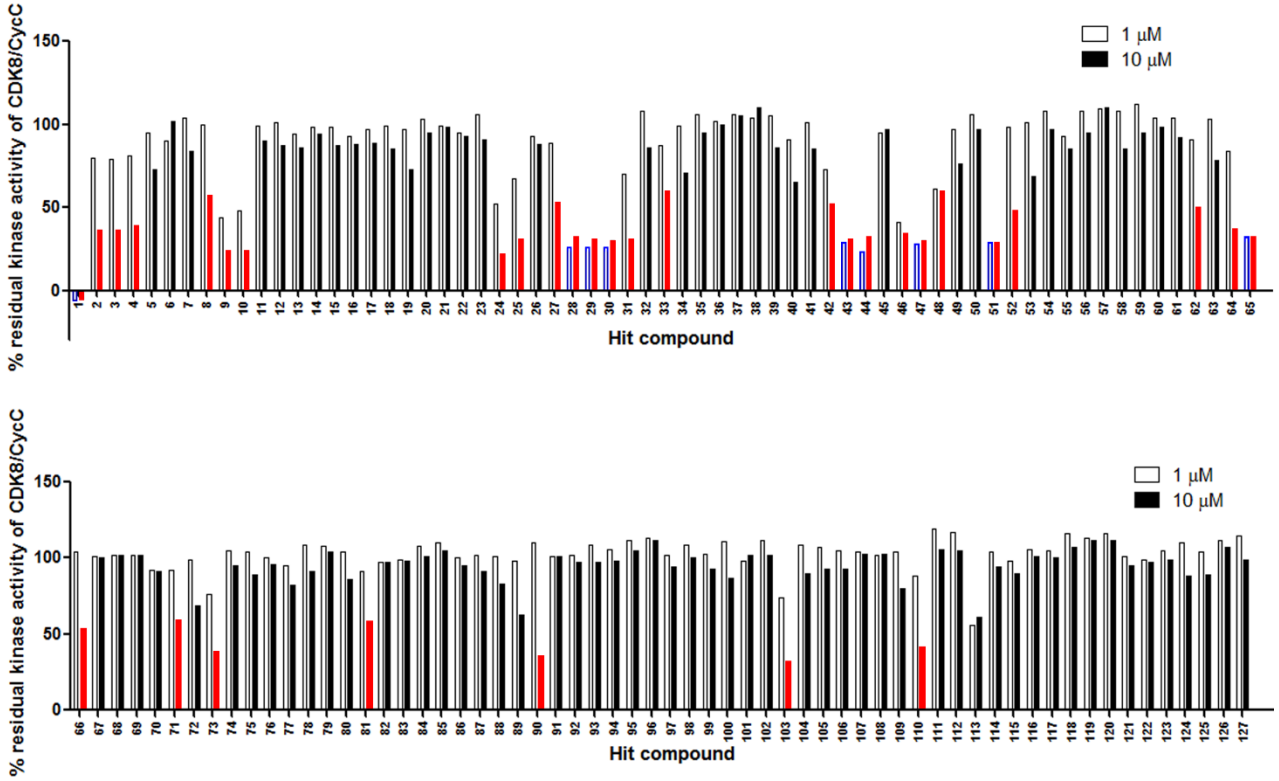

Figure S1. Residual CDK8 kinase activity (as %) after incubation with hit compounds 1-127 at 1 and 10 µM using radiometric ^{33}PanQinase® activity assay. Hit compounds highlighted in blue and red caused less than 35% and 60% residual activity at 1 and 10 µM compound concentration, respectively.

Table S1. Chemical structures of the selected hits and their biological activities.

Compound	Chemical structure	CDK8/CycC			72 h MTT growth inhibition, GI_{50} (μM)			Closest ChEMBL CDK8 inhibitor entry (Similarity)
		% Residual activity at 1 μM		IC_{50} (μM)	Colo 205	HCT 116	HT-29	
		^{33}PanQinase	ADP-Glo	ADP-Glo				
Senexin A	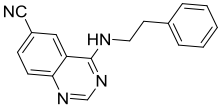	-	-	0.183 ± 0.081	> 15	> 15	> 15	-
sorafenib	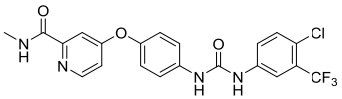	-	-	0.133 ± 0.063	5.65 ± 0.30	5.28 ± 0.14	4.80 ± 0.14	-
Hit 1	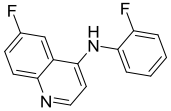	-6.0	25.3	0.386 ± 0.254	11.3 ± 3.26	8.93 ± 0.42	9.01 ± 1.00	CHEMBL2007603 (0.148)
Hit 28	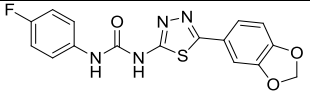	25.0	30.0	0.184 ± 0.049	> 15	8.02 ± 0.37	7.72 ± 1.01	CHEMBL1977134 (0.158)
Hit 29	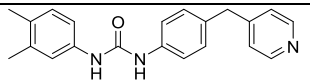	26.0	27.9	0.018 ± 0.003	6.43 ± 0.50	8.56 ± 1.38	8.25 ± 1.22	CHEMBL1336 (0.257)
Hit 30	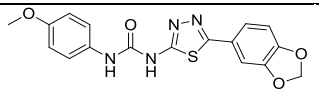	26.0	15.4	0.020 ± 0.009	> 15	8.21 ± 0.39	7.26 ± 0.63	CHEMBL1977134 (0.157)
Hit 43	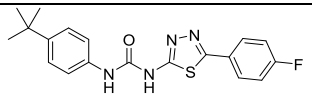	29.0	13.8	0.059 ± 0.001	6.51 ± 0.44	4.92 ± 0.22	6.04 ± 0.03	CHEMBL2007124 (0.152)

Hit 44	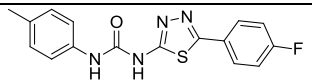	23.0	12.4	0.039 ± 0.011	> 15	9.44 ± 2.87	8.09 ± 1.36	CHEMBL1968606 (0.148)
Hit 47	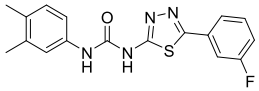	28.0	18.0	0.047 ± 0.016	8.91 ± 0.27	6.71 ± 0.65	6.50 ± 0.26	CHEMBL1336 (0.146)
Hit 51	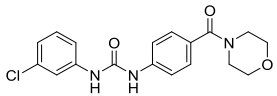	29.0	26.1	0.135 ± 0.090	> 15	> 15	> 15	CHEMBL1968606 (0.377)
Hit 65	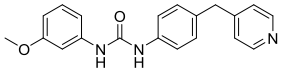	32.0	12.5	0.061 ± 0.034	> 15	> 15	> 15	CHEMBL2007124 (0.283)

Table S2. Mutational status of colorectal cancer cell lines.

Colorectal cancer cell line	Status	Reference
Colo 205	mut APC, mut CTNNB1, CDK8 overexpression	[38, 39]
HCT 116	wt APC, mut CTNNB1, CDK8 overexpression	[12, 38]
HT-29	mut APC, wt CTNNB1, CDK8 overexpression	[12, 38]

Table S3. Cell viability studies on colorectal cancer cells treated with hits using the MTT assay.

Hit compound	72 h GI_{50} (μM)		
	Colo 205	**HCT 116**	**HT-29**
1	11.3 ± 3.26	8.93 ± 0.42	9.01 ± 1.00
2	5.86 ± 0.56	6.20 ± 0.71	7.41 ± 0.18
24	> 15	6.20 ± 0.04	6.48 ± 1.02
28	> 15	8.02 ± 0.37	7.72 ± 1.01
29	6.43 ± 0.50	8.56 ± 1.38	8.25 ± 1.22
30	> 15	8.21 ± 0.39	7.26 ± 0.63
42	> 15	7.83 ± 0.76	6.99 ± 0.98
43	6.51 ± 0.44	4.92 ± 0.22	6.04 ± 0.03
44	> 15	9.44 ± 2.87	8.09 ± 1.36
46	> 15	0.85 ± 0.18	0.84 ± 0.05
47	8.91 ± 0.27	6.71 ± 0.65	6.50 ± 0.26
88	> 15	0.91 ± 0.06	0.75 ± 0.12
90	5.82 ± 0.61	6.56 ± 0.36	6.50 ± 0.52
96	> 15	8.46 ± 0.02	8.83 ± 1.07
100	7.03 ± 0.56	7.20 ± 0.99	5.65 ± 0.87
105	> 15	8.61 ± 0.76	7.84 ± 2.46

References

1. Akoulitchev, S.; Chuikov, S.; Reinberg, D. TFIIH is Negatively Regulated by Cdk8-Containing Mediator Complexes. *Nature* **2000**, 407, 102-106.
2. Donner, A. J.; Ebmeier, C. C.; Taatjes, D. J.; Espinosa, J. M. CDK8 Is a Positive Regulator of Transcriptional Elongation Within the Serum Response Network. *Nat. Struct. Mol. Biol.* **2010**, 17, 194.
3. Fryer, C. J.; White, J. B.; Jones, K. A. Mastermind Recruits CycC:CDK8 to Phosphorylate the Notch ICD and Coordinate Activation with Turnover. *Mol. Cell.* **2004**, 16, 509-520.
4. Donner, A. J.; Szostek, S.; Hoover, J. M.; Espinosa, J. M. CDK8 Is a Stimulus-Specific Positive Coregulator of P53 Target Genes. *Mol. Cell* **2007**, 27, 121-133.
5. Alarcón, C.; Zaromytidou, A.-I.; Xi, Q.; Gao, S.; Yu, J.; Fujisawa, S.; Barlas, A.; Miller, A. N.; Manova-Todorova, K.; Macias, M. J.; Sapkota, G.; Pan, D.; Massagué, J. Nuclear CDKs Drive Smad Transcriptional Activation and Turnover in BMP and TGF-β Pathways. *Cell* **2009**, 139, 757-769.
6. Galbraith, M. D.; Allen, M. A.; Bensard, C. L.; Wang, X.; Schwinn, M. K.; Qin, B.; Long, H. W.; Daniels, D. L.; Hahn, W. C.; Dowell, R. D.; Espinosa, J. M. HIF1A Employs

CDK8-Mediator to Stimulate RNAPII Elongation in Response to Hypoxia. *Cell* **2013**, 153, 1327-1339.
7. Xu, D.; Li, C.-F.; Zhang, X.; Gong, Z.; Chan, C.-H.; Lee, S.-W.; Jin, G.; Rezaeian, A.-H.; Han, F.; Wang, J.; Yang, W.-L.; Feng, Z.-Z.; Chen, W.; Wu, C.-Y.; Wang, Y.-J.; Chow, L.-P.; Zhu, X.-F.; Zeng, Y.-X.; Lin, H.-K. Skp2–MacroH2A1–CDK8 Axis Orchestrates G2/M Transition and Tumorigenesis. *Nat. Commun.* **2015**, 6.
8. Kapoor, A.; Goldberg, M. S.; Cumberland, L. K.; Ratnakumar, K.; Segura, M. F.; Emanuel, P. O.; Menendez, S.; Vardabasso, C.; Leroy, G.; Vidal, C. I.; Polsky, D.; Osman, I.; Garcia, B. A.; Hernando, E.; Bernstein, E. The Histone Variant MacroH2A Suppresses Melanoma Progression through Regulation of CDK8. *Nature* **2010**, 468, 1105.
9. Broude, E. V.; Gyorffy, B.; Chumanevich, A. A.; Chen, M.; McDermott, M. S. J.; Shtutman, M.; Catroppo, J. F.; Roninson, I. B. Expression of CDK8 and CDK8-Interacting Genes as Potential Biomarkers in Breast Cancer. *Curr. Cancer Drug Targets* **2015**, 15, 739-749.
10. Xu, W.; Wang, Z.; Zhang, W.; Qian, K.; Li, H.; Kong, D.; Li, Y.; Tang, Y. Mutated K-Ras Activates CDK8 to Stimulate the Epithelial-to-Mesenchymal Transition in Pancreatic Cancer in Part via The Wnt/β-Catenin Signaling Pathway. *Cancer Lett.* **2015**, 356, 613-627.
11. Pelish, H. E.; Liau, B. B.; Nitulescu, I. I.; Tangpeerachaikul, A.; Poss, Z. C.; Da Silva, D. H.; Caruso, B. T.; Arefolov, A.; Fadeyi, O.; Christie, A. L.; Du, K.; Banka, D.; Schneider, E. V.; Jestel, A.; Zou, G.; Si, C.; Ebmeier, C. C.; Bronson, R. T.; Krivtsov, A. V.; Myers, A. G.; Kohl, N. E.; Kung, A. L.; Armstrong, S. A.; Lemieux, M. E.; Taatjes, D. J.; Shair, M. D. Mediator Kinase Inhibition Further Activates Super-Enhancer-Associated Genes in AML. *Nature* **2015**, 526, 273-276.
12. Firestein, R.; Bass, A. J.; Kim, S. Y.; Dunn, I. F.; Silver, S. J.; Guney, I.; Freed, E.; Ligon, A. H.; Vena, N.; Ogino, S.; Chheda, M. G.; Tamayo, P.; Finn, S.; Shrestha, Y.; Boehm, J. S.; Jain, S.; Bojarski, E.; Mermel, C.; Barretina, J.; Chan, J. A.; Baselga, J.; Tabernero, J.; Root, D. E.; Fuchs, C. S.; Loda, M.; Shivdasani, R. A.; Meyerson, M.; Hahn, W. C. CDK8 is a Colorectal Cancer Oncogene that Regulates β-Catenin Activity. *Nature* **2008**, 455, 547.
13. Firestein, R.; Hahn, W. C. Revving the Throttle on an Oncogene: CDK8 Takes the Driver Seat. *Cancer Res.* **2009**, 69, 7899-7901.
14. Zhao, J.; Ramos, R.; Demma, M. CDK8 Regulates E2F1 Transcriptional Activity through S375 Phosphorylation. *Oncogene* **2013**, 32, 3520-3530.
15. Putz, E. M.; Gotthardt, D.; Hoermann, G.; Csiszar, A.; Wirth, S.; Berger, A.; Straka, E.; Rigler, D.; Wallner, B.; Jamieson, A. M.; Pickl, W. F.; Zebedin-Brandl, E. M.; Muller, M.; Decker, T.; Sexl, V. CDK8-Mediated STAT1-S727 Phosphorylation Restrains NK Cell Cytotoxicity and Tumor Surveillance. *Cell Rep.* **2013**, 4, 437-444.
16. Westerling, T.; Kuuluvainen, E.; Makela, T. P. Cdk8 Is Essential for Preimplantation Mouse Development. *Mol. Cell. Biol.* **2007**, 27, 6177.
17. Powell, S. M.; Zilz, N.; Beazer-Barclay, Y.; Bryan, T. M.; Hamilton, S. R.; Thibodeau, S. N.; Vogelstein, B.; Kinzler, K. W. APC Mutations Occur Early During Colorectal Tumorigenesis. *Nature* **1992**, 359, 235-237.
18. Tetsu, O.; McCormick, F. Beta-Catenin Regulates Expression of Cyclin D1 in Colon Carcinoma Cells. *Nature* **1999**, 398, 422-426.
19. Herbst, A.; Jurinovic, V.; Krebs, S.; Thieme, S. E.; Blum, H.; Goke, B.; Kolligs, F. T. Comprehensive Analysis of Beta-Catenin Target Genes in Colorectal Carcinoma Cell Lines with Deregulated Wnt/Beta-Catenin Signaling. *BMC Genomics* **2014**, 15, 74.
20. FILTER, version 2.0.2, Openeye Scientific Software: Sante Fe, NM. **2010**.
21. Hawkins, P. C.; Skillman, A. G.; Warren, G. L.; Ellingson, B. A.; Stahl, M. T. Conformer Generation with OMEGA: Algorithm and Validation using High Quality Structures

from the Protein Databank and Cambridge Structural Database. *J. Chem. Inf. Model.* **2010**, 50, 572-584.
22. OMEGA, version 2.4.6, Openeye Scientific Software: Sante Fe, NM. **2013**.
23. Sali, A.; Blundell, T. L. Comparative Protein Modelling by Satisfaction of Spatial Restraints. *J. Mol. Biol.* **1993**, 234, 779-815.
24. Shen, M. Y.; Sali, A. Statistical Potential for Assessment and Prediction of Protein Structures. *Protein Sci.* **2006**, 15, 2507-2524.
25. Case, D. A.; Babin, V.; Berryman, J. T.; Betz, R. M.; Cai, Q.; Cerutti, D. S.; Cheatham, T. E.; Darden, T. A.; Duke, R. E.; Gohlke, H.; Goetz, A. W.; Gusarov, S.; Homeyer, N.; Janowski, P.; Kaus, J.; Kolossváry, I.; Kovalenko, A.; Lee, T. S.; LeGrand, S.; Luchko, T.; Luo, R.; Madej, B.; Merz, K. M.; Paesani, F.; Roe, D. R.; Roitberg, A.; Sagui, C.; Salomon-Ferrer, R.; Seabra, G.; Simmerling, C. L.; Smith, W.; Swails, J.; Walker; Wang, J.; Wolf, R. M.; Wu, X.; Kollman, P. A. *Amber 14*, University of California, San Francisco: 2014.
26. ROCS, version 3.1.2, Openeye Scientific Software: Sante Fe, NM. **2011**.
27. Hawkins, P. C.; Skillman, A. G.; Nicholls, A. Comparison of Shape-Matching and Docking as Virtual Screening Tools. *J. Med. Chem.* **2007**, 50, 74-82.
28. OEDocking, version 3.0.0, Openeye Scientific Software: Sante Fe, NM. **2012**.
29. Kelley, B. P.; Brown, S. P.; Warren, G. L.; Muchmore, S. W. POSIT: Flexible Shape-Guided Docking For Pose Prediction. *J. Chem. Inf. Model.* **2015**, 55, 1771-1780.
30. McGann, M. FRED Pose Prediction and Virtual Screening Accuracy. *J. Chem. Inf. Model.* **2011**, 51, 578-596.
31. McGann, M. FRED and HYBRID Docking Performance on Standardized Datasets. *J. Comput. Aided Mol. Des.* **2012**, 26, 897-906.
32. Halgren, T. A.; Murphy, R. B.; Friesner, R. A.; Beard, H. S.; Frye, L. L.; Pollard, W. T.; Banks, J. L. Glide: A New Approach for Rapid, Accurate Docking and Scoring. 2. Enrichment Factors in Database Screening. *J. Med. Chem.* **2004**, 47, 1750-1759.
33. Friesner, R. A.; Banks, J. L.; Murphy, R. B.; Halgren, T. A.; Klicic, J. J.; Mainz, D. T.; Repasky, M. P.; Knoll, E. H.; Shelley, M.; Perry, J. K.; Shaw, D. E.; Francis, P.; Shenkin, P. S. Glide: A New Approach for Rapid, Accurate Docking and Scoring. 1. Method and Assessment of Docking Accuracy. *J. Med. Chem.* **2004**, 47, 1739-1749.
34. Duan, J.; Dixon, S. L.; Lowrie, J. F.; Sherman, W. Analysis and Comparison of 2D Fingerprints: Insights Into Database Screening Performance Using Eight Fingerprint Methods. *J. Mol. Graph. Model.* **2010**, 29, 157-170.
35. Sastry, M.; Lowrie, J. F.; Dixon, S. L.; Sherman, W. Large-Scale Systematic Analysis of 2D Fingerprint Methods and Parameters to Improve Virtual Screening Enrichments. *J. Chem. Inf. Model.* **2010**, 50, 771-784.
36. Baell, J. B.; Holloway, G. A. New substructure filters for removal of pan assay interference compounds (PAINS) from screening libraries and for their exclusion in bioassays. *J Med Chem* **2010**, 53, 2719-2740.
37. Teo, T.; Yu, M.; Yang, Y.; Gillam, T.; Lam, F.; Sykes, M. J.; Wang, S. Pharmacologic Co-Inhibition of Mnks and mTORC1 Synergistically Suppresses Proliferation and Perturbs Cell Cycle Progression in Blast Crisis-Chronic Myeloid Leukemia Cells. *Cancer Lett.* **2015**, 357, 612-623.
38. Ilyas, M.; Tomlinson, I. P.; Rowan, A.; Pignatelli, M.; Bodmer, W. F. Beta-Catenin Mutations in Cell Lines Established from Human Colorectal Cancers. *Proc. Natl. Acad. Sci. U. S. A.* **1997**, 94, 10330-10334.
39. Mallinger, A.; Schiemann, K.; Rink, C.; Stieber, F.; Calderini, M.; Crumpler, S.; Stubbs, M.; Adeniji-Popoola, O.; Poeschke, O.; Busch, M.; Czodrowski, P.; Musil, D.; Schwarz, D.; Ortiz-Ruiz, M.-J.; Schneider, R.; Thai, C.; Valenti, M.; de Haven Brandon, A.; Burke, R.; Workman, P.; Dale, T.; Wienke, D.; Clarke, P. A.; Esdar, C.; Raynaud, F. I.; Eccles,

S. A.; Rohdich, F.; Blagg, J. Discovery of Potent, Selective, and Orally Bioavailable Small-Molecule Modulators of the Mediator Complex-Associated Kinases CDK8 and CDK19. *J. Med. Chem.* **2016**, 59, 1078-1101.